SLAC-PUB-2503
May 1980
(T/E)

TWO-PHOTON COLLISIONS AND QCD*

J. F. Gunion
University of California at Davis
Physics Department, Davis, California 95616

and

Stanford Linear Accelerator Center
Stanford University, Stanford, California 94305

Abstract

A critical review of the applications of QCD to low- and high-p_T interactions of two photons is presented. The advantages of the two-photon high-p_T tests over corresponding hadronic beam and/or target tests of QCD are given particular emphasis.

Results for the two-photon interactions are now becoming available from experiments at PETRA and two-photon experiments at PEP will soon begin. Thus, it seems an opportune time to review and assess the implications of current theoretical ideas, especially of quantum chromodynamics, for photon-photon collisions. Particular emphasis will be placed upon the unique characteristics of a photon target, photon beam combination as compared to the hadron target situation. A brief outline of the talk is:

I) Remarks on low-p_T physics in $\gamma\gamma$ collisions.

II) Review of the salient features of high-p_T hadron target collisions -- problems and ambiguities.

III) High-p_T 2γ physics.

1. Inclusive jet and single particle production
   (a) 2-jet topology.
   (b) 3-jet topology.
   (c) 4-jet topology.
   (d) Higher twist and vector dominance backgrounds, and the importance of single particle spectra.
2. Exclusive reactions.

IV) Conclusions.

I have attempted to keep the number of equations minimal and emphasize physical tests and conclusions. This talk does not cover the deep inelastic photon target situation, reviewed by T. Walsh at this conference.

---

* Work supported in part by the Department of Energy under contract DE-AC03-76SF00515 and the A. P. Sloan Foundation.

(Presented at the International Workshop on Gamma-Gamma Collisions, Universite de Picardie, Amiens, France, April 8 - 12, 1980.)

I. Low-p_T Physics in 2γ Collisions

The fundamental observable in 2γ collisions at low-p_T is the total cross section, $\sigma_{\gamma\gamma}$. Various guesses as to the form of this cross section have appeared in the literature over the years.[1] I will present a point of view which differs slightly from those given earlier.

Most workers agree that $\sigma_{\gamma\gamma}$ cannot be obtained entirely from vector dominance. The photons have additional point-like couplings which presumably yield an addition to $\sigma_{\gamma\gamma}$ above the vector dominance estimate. These point-like couplings can, in particular, lead to fixed-pole ($J = 0$) contributions to the large s limit of $\sigma_{\gamma\gamma}$. A typical vector dominance estimate of $\sigma_{\gamma\gamma}$ would include only the diagrams of Fig. 1. There we employ the Low-Nussinov[2] gluon exchange model for the Pomeron and represent Regge exchanges as due to quark exchange (as in the duality approach) with all possible gluon radiative corrections.

The point-like coupling diagrams of Fig. 2 are not included in the VMD diagrams of Fig. 1. Of course, interference terms between vector-dominated (V) type couplings and point-like (PL) couplings are also possible. An estimate for the Pomeron contribution to $\sigma_{\gamma\gamma}$, which includes both V and PL couplings can be obtained from factorization,

$$\lim_{s\to\infty} \sigma_{\gamma\gamma} = \lim_{s\to\infty} \frac{\sigma^2_{\gamma p}}{\sigma_{pp}} \sim 240 \text{ nb} \qquad (1.1)$$

since the Pomeron contribution to the γp cross section should contain both V and PL γ couplings. Certainly in the gluon-exchange Pomeron model the above result is explicitly correct. An estimate for the Regge contribution[1] from VMD is

$$\sigma_{VV}^{\text{Non-Pomeron}} \sim \frac{270 \text{ nb}}{\sqrt{s(\text{GeV}^2)}} \cdot \qquad (1.2)$$

Experimentally it is clear that such a Regge contribution is too small to describe the data[3] which prefers a fit with

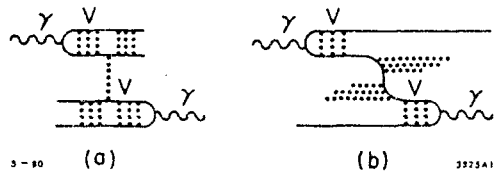

Fig. 1. Vector dominance diagrams for $\sigma_{\gamma\gamma}$: (a) Pomeron or gluon exchange; and (b) Regge exchange, represented by radiatively modified quark exchange.

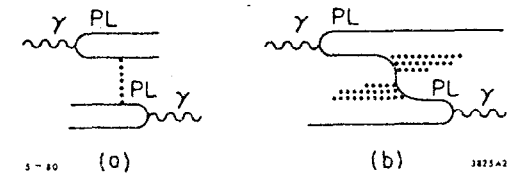

Fig. 2. Purely point-like photon couplings to: (a) the Pomeron; and (b) a typical Reggeon.

$$\sigma_{\gamma\gamma}^{\text{Non-Pomeron}} \sim \frac{840 \text{ nb}}{\sqrt{s(\text{GeV}^2)}} \tag{1.3}$$

or else a smaller Regge term with some $J = 0$ fixed-pole contribution

$$\sigma_{\gamma\gamma}^{\text{Non-Pomeron}} \sim \frac{A}{\sqrt{s}} + \frac{B}{s} \quad . \tag{1.4}$$

Theoretically

$$\sigma_{\gamma\gamma}^{\text{Non-Pomeron}} = \sigma_{VV}^{\text{Non-Pomeron}} + 2\sigma_{V\,PL}^{\text{Non-Pomeron}} + \sigma_{PL\,PL}^{\text{Non-Pomeron}} \tag{1.5}$$

will clearly be larger than the vector-dominance estimate, but cannot be explicitly calculated. It has, however, been suggested that estimates using finite energy sum rules and duality may be possible. One such scheme[1] is to make the fixed-pole plus vector-dominated Regge contributions to $\sigma_{\gamma\gamma}^{\text{Non-Pomeron}}$ dual to the low energy resonances; this implicitly assumes that the point-like photon components couple to resonances but not to Regge terms. It seems more reasonable to me that the point-like photon resonance component is dual to a point-like Regge component. This is illustrated in Fig. 3(a). Corresponding statements apply to mixed vector-dominated and point-like couplings; an example is given in Fig. 3(b). Thus one would maintain a standard form for the finite energy sum rule

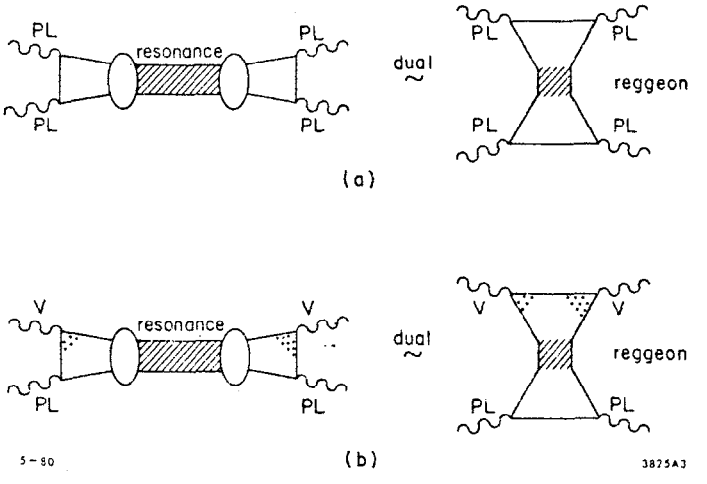

Fig. 3. Duality for $\sigma_{\gamma\gamma}$ -- each $\gamma\gamma \to$ Resonance $\to \gamma\gamma$ diagram has its corresponding Reggeon diagram: (a) for all point-like (PL) couplings; and (b) for a sample mixed PL, vector-dominated (V) coupling diagram.

$$\int_{s_0}^{s_1} \sigma_{\gamma\gamma}^{\text{Resonance}} \frac{ds}{s} = \int_{s_0}^{s_1} \sigma_{\gamma\gamma}^{\text{Regge}} \frac{ds}{s} \tag{1.6}$$

and the fact that the experimentally determined left-hand, resonance side of (1.6) is larger than the contribution to the right-hand side coming from pure vector dominance, $\sigma_{VV}^{\text{Regge}}$ (Eq. (1.2)), is easily explained by the additional $\sigma_{V\,PL}^{\text{Regge}}$ terms of (1.5) which should be included in (1.6). The Regge fit, (1.3), is such that (1.6) is approximately satisfied. Ideally one would like to calculate the left-hand side of (1.6) with high precision (perhaps possible as more resonance data becomes available), determine $\sigma_{\gamma\gamma}^{\text{Regge}}$ from (1.6) (i.e., determine A in Eq. (1.4)) and then use the experimental measurement of $\sigma_{\gamma\gamma}^{\text{Non-Pomeron}}$ to decide if a fixed-pole

contribution (B/s in Eq. (1.4)) is present. Certainly one cannot rule out a small fixed-pole term at the moment. However, there seems to be no obvious justification for identifying the coefficient, B, of the fixed-pole 1/s behavior with the coefficient of 1/s obtained from the simple bare-fermion-loop box diagram. One must consider simultaneously all diagrams with gluon and/or fermion bubble corrections to the bare fermion loop. The $s \to \infty$ limit of the sum of all such diagrams should then be separated into Regge and fixed-pole terms; this calculation is not possible without first essentially solving the confinement problem.

An interesting question is whether there is any direct way of exposing the point-like component of the photon using low p_T observations. In fact most workers[4,5] who have examined the fragmentation $\gamma \to$ fast meson, M agree that a point-like photon component will result in a softer-than-expected spectrum at high x_F $\left(x_F = (E_M + P_M^z)/(E_M + P_M^z)_{max}\right)$:

$$\frac{dN}{dx_F} \sim (1 - x_F)^0 \qquad \text{point-like photon}$$

$$\frac{dN}{dx_F} \sim (1 - x_F)^1 \qquad \text{vector-dominated photon} \quad . \tag{1.7}$$

A sample model[4] is that based on the QCD bremstrahlung diagrams of Fig. 4, which illustrate $\gamma \to$ meson fragmentation at low p_T. Basically, the meson remembers the fractional momentum distribution of quarks in the photon.[6] For a vector-dominated photon[7]

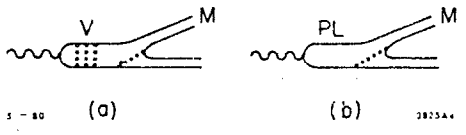

Fig. 4. Bremstrahlung diagrams for $\gamma \to$ meson, M: (a) for the vector-dominated photon; and (b) for the point-like photon.

$$G_{q/\gamma_V}(x) \sim (1-x)^1 \tag{1.8a}$$

whereas for a point-like photon

$$G_{q/\gamma_{PL}}(x) \sim (1-x)^0 \quad . \tag{1.8b}$$

The weaker suppression predicted for a point-like photon is apparently present[9] in $\gamma p \to$ fast meson, M, where $M = \pi^+$ or π^- is observed in the photon fragmentation region. The same photon fragmentation spectrum should be observed in $\gamma\gamma$ collisions.

In summary, even at low p_T, we already have and can expect to find additional evidence in $\gamma\gamma$ collisions for a non-vector-dominated component of the photon. Such evidence is, however, less direct than that which can be obtained from $\gamma\gamma$ collisions at high transverse momentum.

II. Problems and Ambiguities in High-p_T Hadron Collisions

First let us recall the salient features of high-p_T collisions. The typical structure of a high-p_T inclusive jet cross section is illustrated in Fig. 5. It has been proven[10] that, in leading log, the correct procedure is to compute the jet cross section by convoluting p_T^2 dependent distribution functions for the secondaries, a and b coming from A and B respectively, which participate directly in the hard scattering subprocess $a+b \to c+d$, with the cross section for that subprocess: either c or d can form the observed jet. Thus one has for c = jet

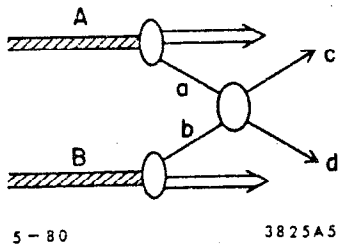

Fig. 5. High-p_T jet production.

$$E_c \frac{d\sigma}{d^3p_c} = \frac{1}{\pi}\int dx_a\, dx_b\, G_{a/A}(x_a, p_T^2)\, G_{b/B}(x_b, p_T^2) \frac{d\sigma^{a+b\to c+d}}{dt'} s'\delta(s'+t'+u') \tag{2.1}$$

where $s' = x_a x_b s$, $t' = x_a t$, $u' = x_b u$, $p_T^2 = \frac{u't'}{s'} = \frac{ut}{s}$, and s, t and u are the Mandlestam invariants appropriate to $A+B \to c+X$. The distribution functions have the standard scale-breaking behavior and can presumably be measured via deep inelastic and/or massive μ-pair production.

The subprocess cross sections $\frac{d\sigma^{a+b\to c+d}}{dt'}$ are computable in the appropriate large s', fixed angle limit in QCD even when some of the participating particles are non-elementary.[11] The general form of the result is,† up to possible anomalous dimension powers of $\log p_T^2/\Lambda^2$,

$$\left.\frac{d\sigma^{a+b\to c+d}}{dt'}\right|_{\substack{\text{fixed}\\ \text{angle}}} \sim \frac{1}{s'^{N-2}} \left[\alpha_s(p_T^2)\right]^{N-2} f_{abcd}(\theta'_{c.m.}) \tag{2.2}$$

where in (2.1) s' is of order $4p_T^2$ and $N = n_a + n_b + n_c + n_d$ is the total number of elementary constituents participating in the subprocess. The strong coupling constant has the standard form

$$\alpha_s(p_T^2) = \frac{4\pi}{\left(11 - \frac{2}{3}n_f\right)\log p_T^2/\Lambda^2} \quad . \tag{2.3}$$

Scaling laws of this type are directly testable in exclusive scattering. For instance, ignoring the α_s variation, one predicts and observes

† Here we use a somewhat simplified expression. In actuality a given QCD diagram has α_s's evaluated at various fractions of p_T^2 (a given internal gluon typically transfers only part of the overall momentum transfer). Strictly speaking, though, such corrections are part of the next-to-leading log correction to the leading log result (2.2).

$$\left.\frac{d\sigma}{dt}\right|_{\substack{\text{fixed}\\ \text{angle}}} \underset{\sim}{s\to\infty} \begin{cases} \frac{1}{s^{10}} ; & pp \to pp \\ \frac{1}{s^{8}} ; & \pi p \to \pi p \\ \frac{1}{s^{7}} ; & \gamma p \to \pi p \\ \frac{1}{s^{6}} ; & \gamma p \to \gamma p \end{cases} \qquad (2.4)$$

In addition, the constituent interchange[12] (CIM) class of QCD diagrams (examples appear in Fig. 6) describe the angular dependence and crossing properties of such exclusive reactions extremely well. The normalizations in most cases have not been computed from first principles yet because of the large number of contributing graphs but the simpler diagrams for the pion and proton form factors have been computed and normalized. As an example consider $G_M^{proton}(Q^2)$. One obtains[13]

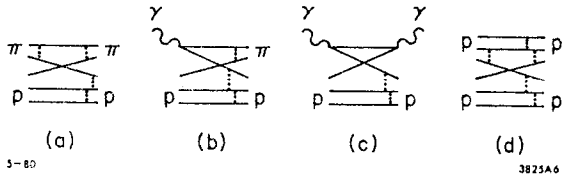

Fig. 6. Examples of CIM type QCD diagrams for: (a) $\pi p \to \pi p$; (b) $\gamma p \to \pi p$; (c) $\gamma p \to \gamma p$; and (d) $pp \to pp$.

$$G_M^{proton}(Q^2) \sim \frac{32\pi^2}{9Q^4}\,\alpha_s^2(Q^2) \sum_{n,m=0}^{\infty} b_{n,m}\left[\log Q^2/\Lambda^2\right]^{-\gamma_n-\gamma_m} \qquad (2.5)$$

where the b_n are computable given certain proton wave function information and γ_n is the standard anomalous dimension appearing in deep inelastic scattering. This expression agrees very well with data provided $\Lambda^2 < .01\ GeV^2$ (i.e., well below the "standard" $\Lambda^2 = .25\ GeV^2$ value). This is illustrated in Fig. 7, taken from Ref. 11.

Focusing for a moment on the reactions involving photons in (2.4), it should be remarked that the experimentally observed decrease in the inverse s power from $1/s^8$ to $1/s^7$ and $1/s^6$ as one proceeds from a reaction involving no photons to ones with one and two photons respectively is direct evidence for the point-like photon component. If the photon were purely vector-dominated $\pi p \to \pi p$, $\gamma p \to \pi p$ and $\gamma p \to \gamma p$ should all have the same fixed-angle s-dependence. Of course, the observed simple power laws should, theoretically, be modified by appropriate powers of $\alpha_s(p_T^2)$, unless α_s is slowly varying as when Λ is small. The requirement of small Λ becomes even more crucial for the $1/s^{10}$ prediction for $pp \to pp$ which agrees well with data but is accompanied by ten powers of $\alpha_s(p_T^2)$. Unless Λ is very small the extra variation with p_T^2 introduced in this way destroys this agreement.

While predictions for exclusive reactions in QCD appear to be successful, ignoring worries about the size of Λ as reflected in the variation of α_s, it is

clear that inclusive reactions have the potential for probing more directly the most elementary QCD reactions such as $qq \to qq$, $qg \to qg$, etc. which with $N = 4$ yield, naively, $1/p_T^4$ behavior in inclusive high p_T scattering (s' in (2.2) converts roughly to $4p_T^2$ in the inclusive cross section (2.1)). Unfortunately, while the subprocesses important in inclusive reactions are simpler the theoretical ambiguities are more numerous. In comparing theory to experiment in the inclusive situation the following problems arise.

(1) The question of the exact subprocess cross section behavior, i.e., the uncertain size of Λ. This is the exact analogue of the exclusive reaction uncertainty.

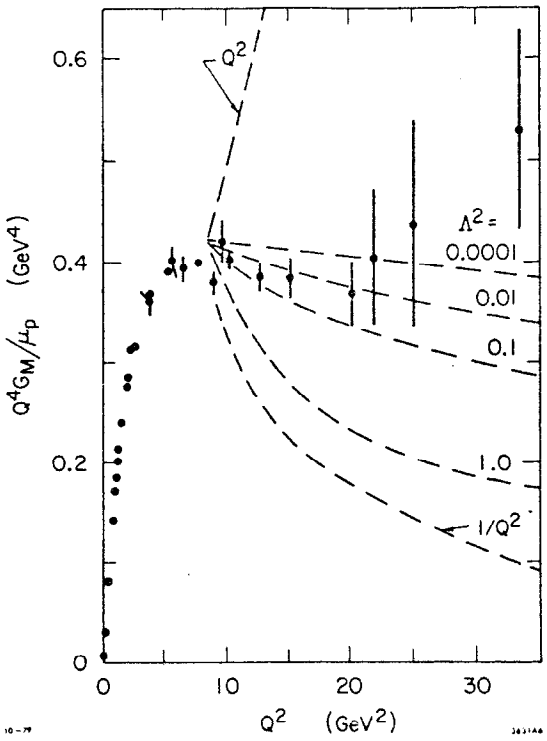

Fig. 7. Prediction for $Q^4 G_M^p(Q^2)$ for various QCD scale parameters Λ^2 (in GeV^2).

(2) Corrections from next-to-leading-log terms, not incorporated in the leading order result ((2.1) + (2.2)). These corrections are in part to the distribution functions in (2.1) and in part to the subprocess cross sections (2.2). The combined next order correction to inclusive jet production via the subprocess $qq \to qq$ has been found to be of order 50%-100%.[14] Next order corrections to the fixed angle predictions (2.4) also occur but have not yet been calculated. The size of all such non-leading-log terms decreases for smaller Λ.

(3) The distribution functions $G_{a/A}$ and $G_{b/B}$ are not so easily determined. Even for a and b being quarks the connection between deep inelastic data and the distribution function is not necessarily straight forward. In particular there are many indications and computations[15] which suggest that higher twist terms are an important component of the observed deep inelastic scale-breaking. This means that the distribution functions extracted from the deep inelastic data could have much less scale breaking than might be naively anticipated when assuming a moderate value of the scale breaking parameter Λ in (2.3). Substantial higher twist contributions lead to a smaller value of Λ as extracted from deep inelastic data and effect the exact shape and normalization of the distribution functions so obtained. Since the higher twist contributions decrease with Q^2 more rapidly than the leading scale-breaking terms an analysis at high Q^2 would not suffer from these ambiguities. Unfortunately this requires large Q^2 values over a large range in $\underline{\log Q^2}$. This is not available; a recent analysis[16] which employs existing neutrino data, with a moderately high low-Q^2 cutoff does, in fact, obtain (with large errors) a lower Λ value than previous analyses, namely $\Lambda = 100 \pm 100$ MeV.

(4) Just as in deep inelastic scattering there may be substantial higher twist contributions to high-p_T particle production.[17] These arise from hard scattering subprocesses, inevitably present in QCD, in which one or more of the participating particles a,b,c,d is non-elementary. A specific model of such higher twist contributions called the "constituent interchange model" has been proposed[17] because of the earlier mentioned success of closely related diagrams for exclusive reactions.

An example of the possible interplay between higher twist and elementary QCD subprocesses is provided by $pp \to \pi X$. There one predicts (in the absence of substantial scale-breaking -- i.e., for small Λ) on the basis of elementary subprocesses such as $qq \to qq$ and higher twist CIM subprocesses such as $qM \to qM$ (M = meson) (Fig. 8)

$$E\frac{d\sigma^{pp\to\pi X}}{d^3p}\bigg|_{90^\circ} \sim \begin{cases} \frac{1}{p_T^4} f(x_T) & qq \to qq \quad \text{etc.} \\ \frac{1}{p_T^8} f'(x_T) & qM \to qM \end{cases} \tag{2.6}$$

where $x_T = 2p_T/\sqrt{s}$ and p_T is the transverse π momentum. The higher twist $qM \to qM$ contribution is only significant because it is enhanced by the so-called trigger bias effect;[18] the particular subprocess $qM \to q\pi$ produces the π meson directly whereas it must appear as a q or g fragment for the more elementary contributions. The effect is a suppression of the elementary-QCD subprocesses relative to the CIM subprocesses by a factor of 10 compared to their relative importance in producing jets.

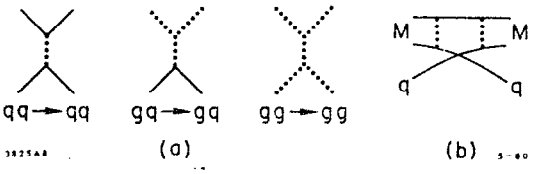

Fig. 8. Examples of QCD subprocess diagrams for: (a) elementary participants-quarks and/or gluons; and (b) $qM \to qM$ where M = meson.

We will return to jets in a moment but let us first look at n_{eff} defined by

$$E\frac{d\sigma^{pp\to\pi X}}{d^3p}\bigg|_{90^\circ} \sim \frac{1}{p_T^{n_{eff}}}\, g(x_T) \quad , \tag{2.7}$$

as extracted from data. A graph[19] obtained from ISR data is shown in Fig. 9. There appears to be a transition from higher n_{eff} powers near 8 to a lower n_{eff} power. If one looks at these $\sqrt{s}$ = 53 GeV/$\sqrt{s}$ = 62 GeV extractions this lower power is probably between 4 and 5. Clearly one might be tempted to say that there is, indeed, a mixture of CIM and elementary-QCD subprocesses. A superposition of the expressions in (2.6) does indeed describe this transition. The scenario is slightly different, however, if Λ is not small but of order Λ = .5 GeV. There is then scale breaking in the quark and gluon distribution functions and non-negligible α_s variation in the elementary-

QCD subprocesses. Both effects tend to increase n_{eff} so that in the experimental energy and x_T range n_{eff} should not have fallen below about 5.5.

In any case, one might be inclined to believe that CIM processes are at least responsible for the $n_{eff} \simeq 8$ region at lower x_T. This unfortunately, is also subject to debate. Feynman and Field[20] and others[21] claim that one should use on-shell quark-quark scattering but incorporate the effects of "smearing" over the intrinsic transverse momentum, k_T, of the quarks in the proton. This procedure requires parameters and cutoffs but probes the $t' \to 0$ singularities of the elementary-QCD $\frac{d\sigma}{dt'}$'s in such a way as to yield high n_{eff} values for these elementary subprocess contributions at moderate p_T. In a Feynman diagram sense, however, the initial quarks or gluons entering the subprocess are necessary off-shell. This off-shellness would shield[22] the above $t' \to 0$ singularity and make it impossible to obtain high n_{eff} values from $qq \to qq$, $qg \to qg$, etc.; higher twist contributions would then be required to explain the lower p_T region of the data. Simultaneously triggering on two high-p_T particles on opposite sides of the beam axis can be shown[23] to eliminate any possible k_T "smearing" effects. As data becomes available regarding such symmetric triggers the question of higher-twist versus smearing as an explanation of moderate p_T data should be resolved. Correlations between the quantum numbers of the two symmetric particle triggers will also serve[23] to discriminate between the possible contributing subprocesses; elementary-QCD subprocesses lead to little correlation while higher twist-CIM subprocesses give rise to substantial correlations.

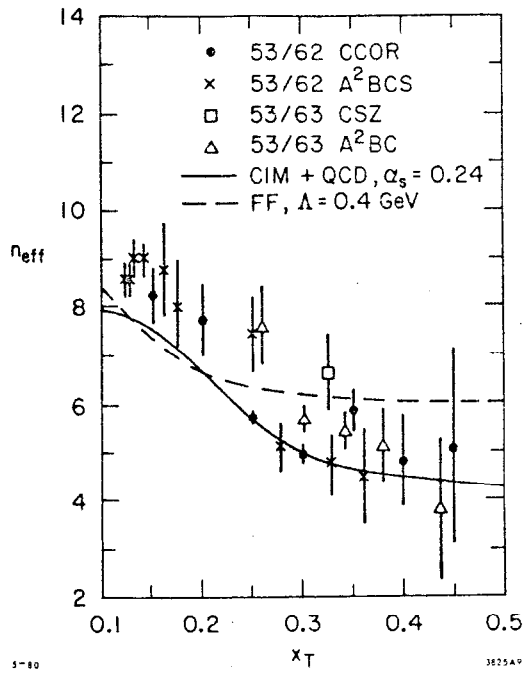

Fig. 9. Effective power n_{eff} dependence on x_T for π^0 production at the ISR. Only the highest energy $\sqrt{s} = 53$ GeV/$\sqrt{s} = 63$ GeV extraction is shown; it probes the highest p_T values. Lower energy extractions, e.g., $\sqrt{s} = 31$ GeV/$\sqrt{s} = 53$ GeV, will always yield higher n_{eff} values since they probe lower p_T values where higher twist terms are more important. Two sample n_{eff} predictions are shown. One uses a superposition of the two terms in (2.6) with no scale breaking. The other is from the Feynman-Field (FF) model with "k_T smearing" and the QCD scale breaking parameter $\Lambda = .4$ GeV.

(5) Which of the many alternatives scenarios for n_{eff} considered above actually holds, if any, is not clear. In addition, there are other difficulties. Both elementary-QCD and CIM subprocesses, especially the latter, have difficulty[24] in describing the ratio

$$\left[E\frac{d\sigma^{\pi^- p\to\pi^- X}}{d^3p}\right]\Big/\left[E\frac{d\sigma^{\pi^- p\to\pi^+ X}}{d^3p}\right] \tag{2.8}$$

as a function of x_T and angle. Both predict that the final π^- is more easily made than the final π^+, i.e., that the quantum numbers of the beam are transmitted to the final particle, especially when produced in the forward direction. The data shows[24] almost no correlation of this type. An additional problem for the CIM is that the phenomenologically successful normalization of the $qM\to qM$ subprocess, obtained from exclusive $\gamma p\to\pi p$ and $\pi p\to\pi p$ scattering data,[17] is much larger than that obtained in a recent calculation[25] using the Brodsky-Lepage techniques.[11] Balancing this is the long standing problem for elementary-QCD subprocesses of their failure to predict the observed behavior

$$E\frac{d\sigma^{pp\to pX}}{d^3p} \sim \frac{1}{p_T^{12}} f(x_T) \tag{2.9}$$

which is a natural result[17] in the CIM due to the existence of the subprocess $qp\to qp$ with fixed angle $1/s^6$ behavior (which translates into the $1/p_T^{12}$ of Eq. (2.9)). The behavior (2.9) suggests that the phenomenologically determined CIM subprocess normalizations are not unreasonable.

(6) As if all the above did not provide sufficient reason for failing to draw firm conclusions from existing high-p_T single particle data a recent "jet" experiment[26] fails to see jets. Only the elementary-QCD subprocesses should contribute significantly to jet cross sections. (The CIM subprocesses are no longer enhanced by the trigger bias effect which results when a single high-p_T particle is triggered on.) Asymptotically as $p_T^{jet}\to\infty$, one should see planar events with four jets, two at high-p_T on opposite sides of the beam axis and two along either beam axis. While the results are preliminary this planar structure is not currently observed when the experiment triggers on a total large transverse energy E_T on one side of the beam. Instead the total E_T is composed of many low-p_T particles in a variety of different azimuthal and rapidity locations. In addition the cross section is more than a factor of 50 above that predicted by the elementary-QCD subprocesses. One guesses that the typical event is not a single high-p_T hard scattering but rather a multiple scattering event, each of the multiple collisions being at low-p_T. Because the trigger is not forcing all the high-p_T momentum to be carried on a single particle (as in the single π trigger), the background has become overwhelming. Or perhaps the theory is wrong. At best, far larger values of E_T are required before the power-law-behaved single-hard-scattering cross sections will stand out above the background.

Even though hadron-hadron collisions producing a high-p_T hadron are still not unambiguously interpretable, it might be that photon + hadron → hadron or hadron + hadron → photon collisions might be beset by fewer problems. To some extent this is the case and it is at least possible to learn from these reactions some facts

which will be relevant when we come to photon-photon collisions. Due to lack of space I will discuss only hadron-hadron collisions with production of a single high-p_T unaccompained photon. There has been an increasing amount of experimental data[27] in this area.

To keep the discussion simple consider the two principle competing processes in pp collisions; an elementary-QCD process $gq \to \gamma q$ yielding $1/p_T^4$ behavior for the inclusive cross section $E_\gamma(d\sigma/d^3p_\gamma)$ and a higher twist (CIM) process $Mq \to \gamma q$ yielding $1/p_T^6$ behavior at fixed x_T. If we compute the γ/π^o ratio it might be anticipated that some of the scale-breaking and other Λ dependent effects might cancel between the γ and π^o predictions. Naively,[28] i.e., for small Λ one obtains as $p_T \to \infty$, $x_T = 2p_T/\sqrt{s}$ fixed

$$\frac{E_\gamma \dfrac{d\sigma^{pp\to\gamma X}}{d^3p_\gamma}}{E_\pi \dfrac{d\sigma^{pp\to\pi X}}{d^3p_\pi}} \propto \begin{cases} \dfrac{1}{(1-x_T)^{1 \text{ or } 2}} & \text{elementary-QCD} \\ p_T^2 & \text{higher twist-CIM} \end{cases} . \qquad (2.10)$$

If elementary-QCD processes dominate both γ and π^o production the γ/π^o ratio should be p_T independent at fixed x_T and a decreasing function of $\sqrt{s}$ at fixed p_T. If higher twist (CIM) diagrams dominate both reactions the γ/π^o ratio should behave as p_T^2 (compare $1/p_T^6$ for $Mq \to \gamma q$ to $1/p_T^8$ for $Mq \to \pi^o q$) with little or no x_T (i.e., $\sqrt{s}$) dependence at fixed p_T. Including other less important subprocesses does not essentially alter the above comparison.

Experimentally the latest ISR data,[27] which compares $\sqrt{s}$ = 31, 45 and 63 GeV, indicates a result much nearer the naive CIM expectation, see Fig. 10. The normalization of the γ/π^o ratio is roughly a factor of 2 below that originally predicted in Ref. 28, i.e., within the anticipated phenomenological normalization uncertainties. However, to a small extent "scale breaking"[29] and to a much larger extent "low k_T smearing"[30] do not entirely cancel out of the γ/π^o ratio. In addition Brodsky and I[31] have completed a preliminary computation of the $Mq \to \gamma q$ subprocess normalization in terms of the PCAC constant, f_π, following the techniques of Ref. 11 and find a result consistent with the $qM \to qM$ results of Ref. 25 -- namely a much smaller normalization than obtained by the earlier phenomenological techniques.[17,28] Thus, the interpretation of hadron-hadron production of high-p_T γ's even though relatively simpler than production of hadrons at high-p_T remains uncertain at this point in time. There is strong evidence for the point-like photon component but the precise subprocess mechanism by which it enters is not yet clear. Where, then, do we turn in order to obtain direct experimental verification of the existence of the most elementary QCD reactions, such as

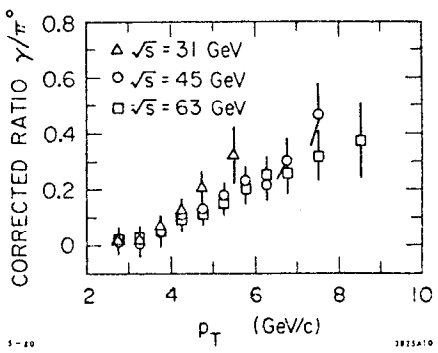

Fig. 10. Comparison of $\sqrt{s}$ = 31, 45 and 63 GeV data for γ/π^o at high-p_T. Data is from M. Diakonov et al., Ref. 27.

quark-quark scattering, and direct experimental information on the normalization of higher twist subprocesses? It appears that photon-photon collisions at high-p_T provide a much less ambiguous probe of both types of subprocess.

III. High-p_T Production in Photon-Photon Reactions[32-36]

III.1. Inclusive Jet and Single Particle Production

We now turn to a discussion of photon-photon collisions producing a high-p_T hadron or jet. Such reactions provide a probe of the same subprocesses as discussed in Section II, elementary-QCD and higher twist-CIM, but will be much less ambiguous in their interpretation. For the calculable point-like photon component: (a) there are many reactions which are predicted to be Λ independent in leading order; (b) there are no hadron wave function, smearing, etc. ambiguities; (c) all subprocess and wave function normalizations are explicitly calculable; (d) the contributions coming from the vector-dominated component of the photon can be shown to be small in most situations; and (e) in addition, different types of subprocesses can often be distinguished through their final state topology. We will divide up the high p_T 2γ subprocesses according to final state topology.

A. 2-Jet Processes[32-36]

In two-photon collisions the simplest subprocess is that illustrated in Fig. 11, $\gamma\gamma \to q\bar{q}$. The final state is exactly the same as that produced via annihilation (aside from the e^+ and e^- spectators) except that the q and $\bar{q}$ jets do not carry the full energy of the incoming e^+ and e^-. The same type of diagram can, of course, be drawn for $e^+e^- \to e^+e^-\mu^+\mu^-$. If the intermediate quark propagator in $\gamma\gamma \to q\bar{q}$ behaves just like the elementary muon propagator in $\gamma\gamma \to \mu^+\mu^-$ then the $\gamma\gamma \to q\bar{q}$ process yields (using the equivalent photon approximation)

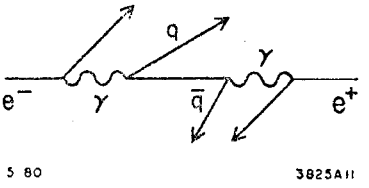

Fig. 11. High-p_T q, $\bar{q}$ production via the subprocess $\gamma\gamma \to q\bar{q}$.

$$E_{Jet}\frac{d\sigma^{ee\to eeJet}}{d^3p_{Jet}} \sim \left(\frac{\alpha}{2\pi}\ell n\,\eta\right)^2 \frac{\alpha^2}{p_T^4} f\left(x_R^{Jet}, \theta_{c.m.}^{Jet}\right) \qquad (3.1)$$

where $x_R = E_{Jet}/E_e$ and

$$\eta = \begin{cases} \dfrac{s}{4m_e^2} & \text{no electron tag} \\ \dfrac{\theta^2_{max}}{\theta^2_{min}} & \text{tagged electron} \end{cases} . \qquad (3.2)$$

As in annihilation it is convenient to compare directly to the analogous μ-pair cross section. We obtain

$$\frac{d\sigma(e^+e^- \to e^+e^- q\bar{q})}{d\sigma(e^+e^- \to e^+e^- \mu^+\mu^-)} = R_{\gamma\gamma} \tag{3.3}$$

with

$$R_{\gamma\gamma} = 3\sum e_q^4 \left(1 + \mathcal{O}(\alpha_s/\pi)\right) \quad . \tag{3.4}$$

For standard fractional charges and two flavor generations $R_{\gamma\gamma} = 34/27$ in leading order. In a model where the photon has a color singlet and a color octet component but experiments are done below color threshold, it is still possible[37] that the octet components of the initial photons could mix together to yield a final state color singlet and yield a much higher value, namely $R_{\gamma\gamma} = 10/3$. In such a model the quark charges are integral above color threshold.

A useful characterization of the magnitude of the two-jet cross section is its contribution to the standard R value of e^+e^- annihilation. Figure 12 from Ref. 34 shows that the contribution ΔR (in the fractional charge model) from all $e^+e^- \to e^+e^- q\bar{q}$ events with $p_T^{quark} > p_T^{min}$ can be very substantial, especially at LEP energies, even for quite large values of p_T^{min}. In the PEP-PETRA range, at $\sqrt{s}$ = 30 GeV, one finds

$$(\Delta R)_{p_T^{min}} = \frac{5}{\left[p_T^{min}(\text{GeV}/c)\right]^2} \tag{3.5}$$

i.e., such processes occur at a rate which is 30% of that for $e^+e^- \to \mu^+\mu^-$ when p_T^{min} = 4 GeV.

As for the usual annihilation R, $R_{\gamma\gamma}$ has $\mathcal{O}(\alpha_s/\pi)$ corrections coming from virtual and real gluon radiation. One anticipates that these will be of the same order as found for R (≈10%). A calculation[38] of the virtual part of the corrections appears to confirm this expectation.

The following important points should be noted.

(1) Production of two jets (and only two jets) is significant only if the point-like γ component is present. The cross section for two vector meson dominated photons to collide producing two and only two jets is small. More often residues in the beam directions remain as discussed in Section II. A more precise vector-dominance

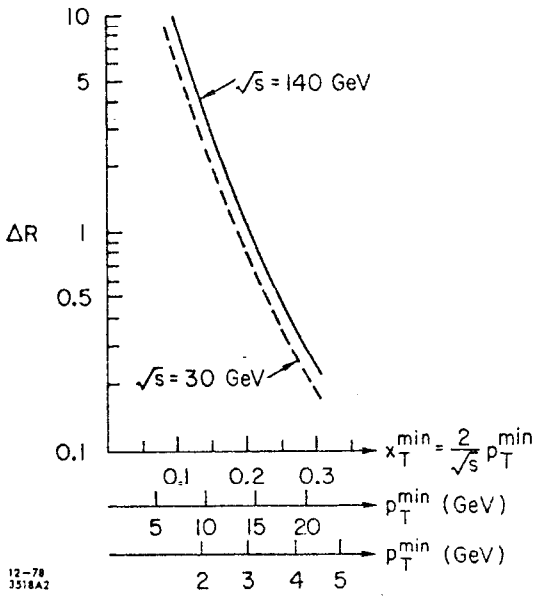

Fig. 12. The contribution to R from $\gamma\gamma \to q\bar{q}$ two-jet processes at $\sqrt{s}$ = 30 and 140 GeV (from Ref. 34).

background estimate appears later, it is basically a higher twist contribution with strong inverse p_T damping.

(2) A failure to see these purely two-jet events implies that perturbative ideas cannot be applied to short distance physics. This would represent a dramatic breakdown of the general approach to short distance reactions motivated by asymptotic freedom.

In fact, two of the PETRA groups, PLUTO and TASSO, have now seen[39] a few two-jet events with one tagged electron. Such tagging eliminates a possibly important background, discussed in Ref. 34, from annihilation events with two bremsstrahlung photons. As the statistics improve we can clearly expect to either confirm or disprove the perturbative predictions based on Fig. 11.

There is a second process, $\gamma\gamma \to gg$, Fig. 13, which produces events with exactly two gluon jets. The diagram involves a fermion loop and occurs at order $(\alpha_s/\pi)^2$. It might be anticipated that it would be negligible; however, explicit calculations[40,41] show that

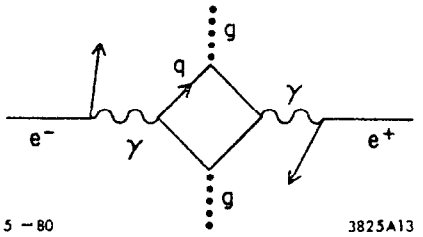

Fig. 13. Production of two high-p_T gluon jets via $\gamma\gamma \to gg$.

$$\frac{E\left(d\sigma^{ee \to ee \text{ gluon jet}}/d^3p\right)}{E\left(d\sigma^{ee \to ee\ q \text{ or } \bar{q} \text{ jet}}/d^3p\right)} \approx .1 \qquad (3.6)$$

essentially independent of x_T and angle. Because of their similar angular dependence, kinematics cannot be used to separate gluon jets from quark jets. The only physically distinguishable features of a gluon jet in this case will be (a) the anticipated higher average multiplicity of gluon jets;[42] (b) the broader transverse spread of a gluon jet;[43] and (c) the polarization of the gluons.[44] With regard to the latter, Ref. 44 shows that even for unpolarized initial photons the gluons are preferably produced with polarization parallel ($\parallel$) to the scattering plane as opposed to perpendicular ($\perp$). They find that

$$P(\theta) \equiv \frac{d\sigma_\perp - d\sigma_\parallel}{d\sigma_\perp + d\sigma_\parallel} \qquad (3.7)$$

becomes as large as -0.3 at $\theta_{c.m.}^{gluon} = 90^o$. This polarization is, however, only indirectly reflected in an oblateness of the gluon jet.[45]

B. 3-Jet Processes[32-35]

This next category of high p_T reactions is distinguished by having two high p_T jets and one beam direction jet in the final state. Elementary QCD subprocesses which produce such a configuration are shown in Fig. 14; they are (a) $\gamma q \to gq$ and (b) $\gamma g \to q\bar{q}$. In two photon collisions these subprocesses yield one and only one beam jet. The beam jet comes from the remnants of the photon which provides the quark or gluon initiating the subprocess. The generic form of the cross section for production

of a high-p_T jet is, in the two cases

$$E\frac{d\sigma^{Jet}}{d^3p} \sim \begin{cases} \frac{1}{\pi}\int dx_\gamma dx_q \; G_{\gamma/e}(x_\gamma)\; G_{q/e}(x_q, p_T^2)\; \frac{d\sigma^{\gamma q \to gq}}{dt'}\; s'\delta(s'+t'+u') & (3.8a) \\ \frac{1}{\pi}\int dx_\gamma dx_g \; G_{\gamma/e}(x_\gamma)\; G_{g/e}(x_g, p_T^2)\; \frac{d\sigma^{\gamma g \to q\bar{q}}}{dt'}\; s'\delta(s'+t'+u') & (3.8b) \end{cases}$$

where we have used the leading log result (2.1) and (2.2). The difference between this situation and the hadron target/beam case is that all the above distribution functions are explicitly calculable. The form of $G_{\gamma/e}$ is obtained[46] from QED and the triggering conditions of the final electron. The distributions $G_{q,g/e}$ are obtained by convolution from

$$G_{q,g/e}(x,p_T^2) = \int_x^1 \frac{dz}{z}\, G_{q,g/\gamma}\left(\frac{x}{z}, p_T^2\right) G_{\gamma/e}(z) \quad . \tag{3.9}$$

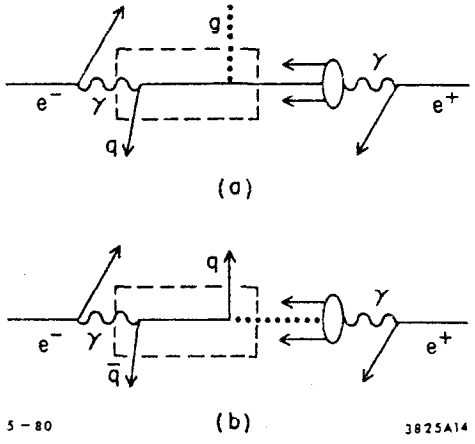

Fig. 14. Elementary-QCD processes with 3-jet final state topology. The --- box encloses the high-p_T subprocess.

Here the non-trivial $G_{q,g/\gamma}$ distribution, which will develop a p_T^2 dependence, is completely calculable, for the point-like photon component. The leading log results were obtained originally by Witten[47] and were rederived diagrammatically in Refs. 6, 33, and 48. More recently the next order corrections have been obtained[49] and do not greatly modify the leading log results in the moderate x range. The form of the leading log result is shown in Fig. 15. (For a more detailed discussion, see T. Walsh's talk at this conference or W. Frazer's and W. Bardeen's talks at the Lake Tahoe Conference.[50]) Both these distributions take the leading log form

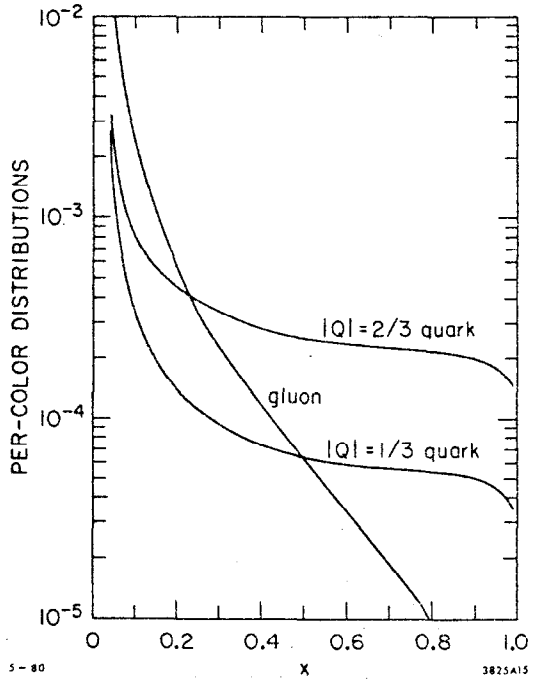

Fig. 15. Plotted are leading log quark and gluon distributions $G_{q/\gamma}(x,"Q^2")$ and $G_{g/\gamma}(x,"Q^2")$ divided by $\log "Q^2"/\Lambda^2$.

$$G_{\begin{bmatrix} q \\ g \end{bmatrix}/\gamma}(x,"Q^2") = \frac{\alpha}{\alpha_s("Q^2")} \begin{bmatrix} q(x) \\ g(x) \end{bmatrix} \tag{3.10}$$

where "Q^2" represents the momentum scale of the short distance probe; in our case "Q^2"

is of order p_T^2. (Written in terms of $1/\alpha_s$, this form also incorporates $\ell n\, \ell n\, "Q^2"/\ell n\, "Q^2"$ corrections to α_s.) The important feature is the factorization of the "Q^2" and x dependences; both increase as $\log\, "Q^2"/\Lambda^2$. In addition g(x) and especially q(x) have much weaker fall off as $x \to 1$ than comparable distributions for the vector-dominated component of the photon (see Ref. 6, for example). Thus the high-p_T situation (in which "Q^2" is of order p_T^2 and x is of order x_T) is dominated by the point-like component of the photon distribution functions.

The subprocess cross sections for $\gamma q \to gq$ and $\gamma g \to q\bar{q}$ are, of course, also explicitly calculable.[32,34] Both take the form

$$\left.\frac{d\sigma}{dt'}\right|_{\substack{\text{fixed}\\ \text{angle}}} = \frac{\alpha_s(p_T^2)}{p_T^4} f(\theta'_{c.m.}) \tag{3.11}$$

where $\theta'_{c.m.}$ is the center-of-mass scattering angle of the final quark or gluon jet (in the γq or γg c.m. frame) and p_T its transverse momentum; $f(\theta'_{c.m.})$ is, of course, different for the two reactions. Combining Eqs. (3.8)-(3.11) we see that $\alpha_s(p_T^2)$ cancels between $d\sigma/dt'$ and $G_{\begin{bmatrix} q \\ g \end{bmatrix}/\gamma}$ and that the jet cross section is completely scale invariant in leading log:

$$E\frac{d\sigma^{Jet}}{d^3p} \sim \frac{1}{(p_T^{Jet})^4} F\left(x_R^{Jet}, \theta_{c.m.}^{Jet}\right) \tag{3.12}$$

where $x_R^{Jet} = E_{Jet}/E_e$ and $\theta_{c.m.}^{Jet}$ is the overall center-of-mass jet scattering angle. The function F is completely determined by the convolution integrals in Eq. (3.8). The $\gamma q \to gq$ contribution is generally larger than the $\gamma g \to q\bar{q}$ contribution because $g(x) < q(x)$ (Fig. 15) over much of the x range.

In Fig. 16 we compare, at $\theta_{c.m.}^{Jet} = 90^\circ$, the cross section $E(d\sigma^{Jet}/d^3p)$ for jet production due to the 3-jet processes, $\gamma q \to gq$ and $\gamma\bar{q} \to g\bar{q}$, to that coming from the $\gamma\gamma \to q\bar{q}$ and $\gamma\gamma \to gg$ 2-jet processes. As expected $d\sigma(3\text{-jet}) < d\sigma(2\text{-jet})$. Clearly, in order to see a subprocess like $\gamma q \to gq$ over the $\gamma\gamma \to q\bar{q}$ subprocess, it is necessary to distinguish the 3-jet from the 2-jet topology.

The fact that there are only two 3-jet processes at the elementary-QCD level makes it possible to also imagine testing the associated predictions[51] for energy distribution in the beam jet and for angular distributions of the opposite side jet relative to the trigger jet. But the most crucial observation is that in leading log none of the Λ dependent complexities associated with hadron targets arise. These elementary-QCD subprocesses yield a α_s, and hence Λ, independent answer in leading order.[52] Next-to-leading log corrections need to be computed for these jet cross sections but are probably no larger than those found in hadron target scattering.

C. 4-Jet Processes[32-35]

Examples of subprocesses which contribute to the 4-jet topology (2 balancing high-p_T jets and 2 beam direction jets) at the elementary QCD level are shown in Fig. 17. Of course, many diagrams and processes are not shown. Note that since the point-like-photon quark distribution, $q(x)$, is so much larger (Fig. 15) than the gluon distribution, $g(x)$, the subprocesses $qq \to qq$, $q\bar{q} \to q\bar{q}$ and $\overline{qq} \to \overline{qq}$ dominate.

The generic form of the cross section from the $qq' \to qq'$ subprocess is

$$E\frac{d\sigma^{Jet}}{d^3p} \sim \frac{1}{\pi}\int dx_q\, dx_{q'}\, G_{q/e}(x_q,p_T^2) \times G_{q'/e}(x_{q'},p_T^2)\,\frac{d\sigma^{qq'\to qq'}}{dt'}\, s'\delta(s'+t'+u') \tag{3.13}$$

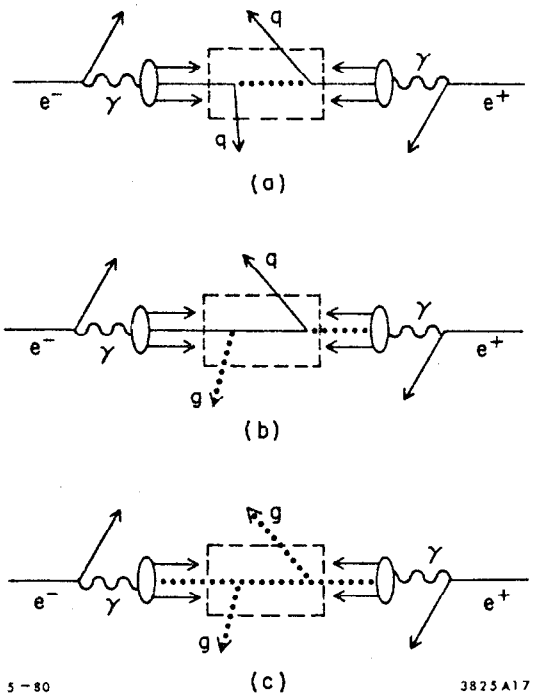

Fig. 17. Examples of elementary-QCD subprocesses contributing to the 4-jet topology: (a) $qq \to qq$; (b) $qg \to qg$; and (c) $gg \to gg$. The order is one of decreasing importance as the gluon distribution for the point-like photon is generally smaller than the quark distribution.

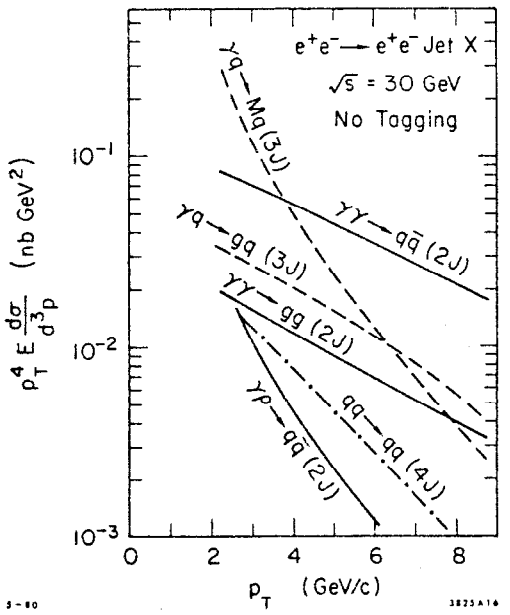

Fig. 16. A comparison of $E\frac{d\sigma^{Jet}}{d^3p}\Big|_{\theta_{c.m.}=90^o}$ coming from various 2-jet (——), 3-jet (---), and 4-jet (-·-·) processes. Except for the $\gamma p \to q\bar{q}$ curve all subprocess contributions are calculated using the point-like photon component only; in particular initial quarks are obtained from the p_T^2 dependent point-like photon distribution. In the curves labeled $\gamma q \to Mq$, $\gamma q \to gq$ and $qq \to qq$ we have also included the antiquark contributions $\gamma\bar{q} \to M\bar{q}$, $\gamma\bar{q} \to g\bar{q}$ and $q\bar{q} \to q\bar{q}/\overline{qq} \to \overline{qq}$, respectively.

with $G_{q/e}G_{q'/e} \propto \left[1/\alpha_s(p_T^2)\right]^2$, see Eq. (3.10), and, from (2.2),

$$\frac{d\sigma^{qq'\to qq'}}{dt'} \sim \frac{1}{p_T^4}\,\alpha_s^2(p_T^2)\,f^{qq'\to qq'}(\theta'_{c.m.}). \tag{3.14}$$

Thus the $\alpha_s(p_T^2)$'s cancel and one obtains

$$\left(E\frac{d\sigma^{Jet}}{d^3p}\right)_{qq'\to qq'} \sim \frac{1}{p_T^4}\,F^{qq'\to qq'}\left(x_R^{Jet},\theta_{c.m.}^{Jet}\right) \tag{3.15}$$

As in the 3-jet case $F^{qq'\to qq'}$ is completely

calculable and scale invariant; in leading order the Λ dependence and other ambiguities which plague the hadron target case are absent. Of course, all the other elementary-QCD subprocesses combine with their appropriate quark/gluon distribution functions in the convolution integral so that this same $\alpha_s(p_T^2)$ cancellation occurs. The $(qq\to qq) + (q\bar{q}\to q\bar{q}) + (\bar{q}\bar{q}\to\bar{q}\bar{q})$ subprocess contribution to $E(d\sigma^{Jet}/d^3p)$ is shown in Fig. 16. Again we have the natural ordering $d\sigma(4\text{-jet}) < d\sigma(3\text{-jet}) < d\sigma(2\text{-jet})$. Note, however, that this is not an ordering in α_s (the α_s's always cancel). Rather the ordering reflects the "directness" with which the final jet is produced; those subprocesses which "waste" energy in the beam direction are suppressed relative to those with less beam direction loss.

Another global picture is provided by Fig. 18 from Ref. 34. There we plot

$$p_T^4 \left.\frac{d\sigma}{dy_1\, dy_2\, d^2p_T}\right|_{y_1=y_2=0,\ p_T^1=p_T^2=p_T}$$

where we imagine triggering on two jets, back-to-back at 90° with equal p_T's. This plot incorporates all subprocesses of the elementary-QCD type which contribute to the various jet topologies.

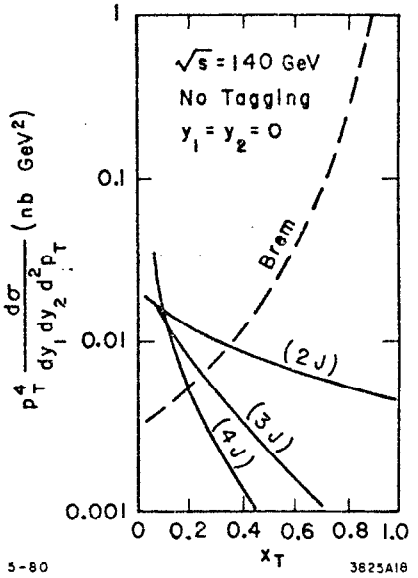

Fig. 18. LEP energy plot of the complete double jet trigger cross sections coming from elementary-QCD processes of each topology type. Also shown is the double bremsstrahlung background which can be eliminated by single tagging, see Ref. 34.

D. Higher Twist and Vector-Dominance Effects -- Single Particle Spectra

(a) Higher Twist and Single Particle Spectra

At this point the alert reader might ask if there are not some higher twist diagrams which complicate the high-p_T jet situation. The answer, fortunately, is in general "no." Only one such diagram is likely to be important. It contributes to the 3-jet case and is based on the subprocess $\gamma q \to Mq$ (the reversal of which was discussed in Section II). The center-of-mass diagram, Fig. 19, is exactly analogous to that drawn for $\gamma q \to gq$, Fig. 14, but with the gluon replaced by a meson. As discussed in Section II, the $\gamma q \to Mq$ subprocess yields $1/p_T^6$ behavior compared to $1/p_T^4$ behavior for the $\gamma q \to gq$ subprocess:

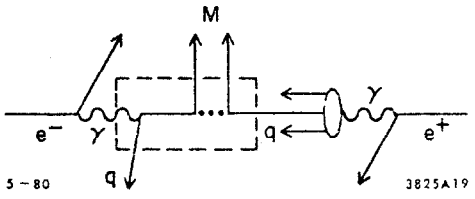

Fig. 19. Higher twist 3-jet topology diagram based on the subprocess $\gamma q \to Mq$.

$$\frac{d\sigma^{\gamma q\to Mq}}{dt'} \sim \frac{\alpha_s^2(p_T^2)}{p_T^6}\,\hat{f}(\theta'_{c.m.}) \qquad (3.16)$$

with $\hat{f}$ completely calculable aside from its

normalization. Either the final meson or final quark can yield an observed "jet;" if the "jet" derives from the meson it will have limited multiplicity and should reconstruct to a resonance. The form of the cross section is

$$E\frac{d\sigma^{Jet}}{d^3p} \sim \frac{1}{\pi}\int dx_\gamma\, dx_q\, G_{\gamma/e}(x_\gamma)\, G_{q/e}(x_q, p_T^2)\, \frac{d\sigma^{\gamma q \to Mq}}{dt'}\, s'\delta(s'+t'+u')$$

$$\sim \frac{1}{p_T^6}\, \alpha_s(p_T^2)\, \hat{F}\left(x_R^{Jet},\ \theta_{c.m.}^{Jet}\right) \quad . \tag{3.17}$$

The function $\hat{F}$ is completely determined by the above convolution integral and $\hat{f}$ of Eq. (3.16). Thus only its normalization is uncertain. This normalization is of great theoretical interest.

The normalization of $\hat{f}(\theta'_{c.m.})$, i.e., of $\gamma q \to Mq$, has been determined phenomenologically[17,32] in a variety of different ways. The crucial ingredient is the normalization of the meson wave function. This has been obtained from:

(a) $\pi p \to \pi p$ elastic scattering which in the CIM is normalized by the proton form factor and the π wave function.

(b) $Mq \to \pi q$ exclusive scattering, the normalization of which is determined by the size of the CIM contribution to $pp \to \pi X$ at high-p_T.

(c) $Mq \to \gamma q$, the normalization of which is determined by the size of the CIM contribution to $pp \to \gamma X$.

All three determinations are completely consistent with one another. For instance if $\pi p \to \pi p$ elastic scattering is used to determine the normalization of the meson wave function, then the higher twist CIM diagrams based on the subprocesses $Mq \to \pi q$ and $Mq \to \gamma q$ yield excellent fits to $pp \to \pi X$ and $pp \to \gamma X$ high-p_T data, respectively. It is also possible to calculate the meson wave function normalization using the techniques of Ref. 11.[31] A much smaller normalization is obtained; but it is difficult to ignore the phenomenological successes (a)-(c). Thus a clean determination of the normalization of $\hat{f}(\theta'_{c.m.})$ is highly desirable.

In Fig. 16 we compare the CIM 3-jet process contribution to jet production at $\theta_{c.m.}^{Jet} = 90^\circ$ to those previously discussed -- using the normalization of (a)-(c) above. Only at lower p_T values does the CIM process clearly dominate the 3-jet topology contribution to jet production.

However, as mentioned in Section II, if we trigger on a single fast meson, e.g., a π^+, then the $\gamma q \to \pi^+ q$ subprocess can produce the π^+ directly whereas the $\gamma q \to gq$ and $\gamma g \to q\bar{q}$ subprocesses as well as the much more important $\gamma\gamma \to q\bar{q}$ subprocess must create the π^+ as a fragment of a quark or gluon. The jet cross section from the $\gamma q \to Mq$ subprocess is roughly a factor of 20 above the direct π^+ cross section (a factor 10 is due to the restriction to $M = \pi^+$ compared to arbitrary M and a factor of 2 from loss of the q jet triggering possibility). In comparison $\gamma\gamma \to q\bar{q}$ with q or $\bar{q}$ fragmenting to the π^+ is suppressed by roughly a factor of 100 relative

to its jet cross section, mostly because of the trigger bias effect.[18] Thus there is a relative enhancement of the CIM subprocess by a factor of 5 in the single π^+ trigger situation. The three most important single pion spectrum contributions are given in Fig. 20 (at $\theta^{\pi^+}_{c.m.} = 90^o$) where it is seen that the CIM term dominates over the p_T range shown, if the normalization from (a)-(c) is employed.

Preliminary "single tag" spectra for $\left(dN^{ee \to ee\pi X}/dp_T^2\right)$ have been obtained by both TASSO and PLUTO.[39] Both exhibit a sharp break at $p_T^2 \approx 1$ (GeV/c)^2 and a large high-p_T tail. A detailed study of these spectra should clearly determine whether or not there is room for a large CIM contribution; triggering efficiencies, etc., must be unfolded before comparison to theory can be made.

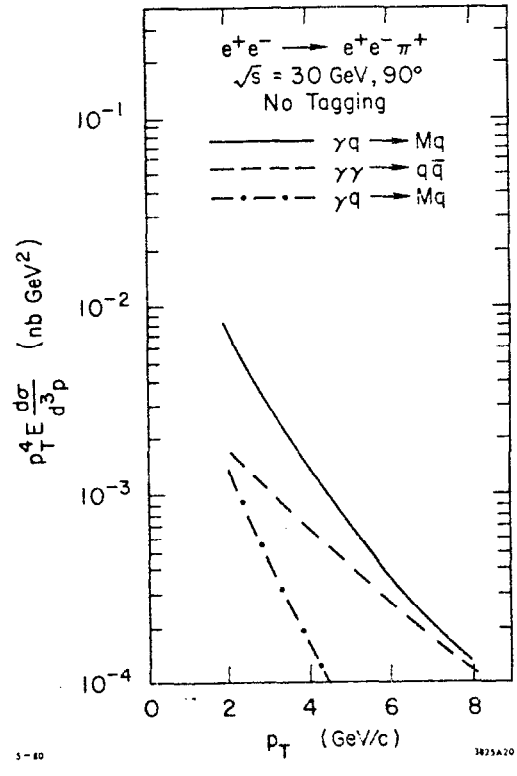

Fig. 20. Contributions to π^+ production at 90° from: (a) $\gamma q \to \pi^+ q$ where the q comes from the point-like photon component; (b) $\gamma\gamma \to q\bar{q}$ with either the q or $\bar{q}$ fragmenting to the observed π^+; (c) $\gamma q \to \pi^+ q$ where the initial q comes from the vector-dominated photon component.

(b) Vector Dominance Backgrounds

In Figs. 16 and 20 we have also plotted the largest vector dominance backgrounds, to jet and single π^+ production respectively. In the jet case we have compared the 2-jet contribution coming from the subprocess $\gamma\rho \to q\bar{q}$ (i.e., one of the initial two photons is vector dominated as shown in Fig. 21a) to the purely point-like diagram based on $\gamma\gamma \to q\bar{q}$. The process $\gamma\rho \to q\bar{q}$ is a higher-twist relative of $\gamma\gamma \to q\bar{q}$ yielding $1/p_T^6$ vs. $1/p_T^4$ behavior for the jet cross section. Not surprisingly it is very much suppressed. This is typical of vector dominance backgrounds. For a given topology (2, 3 or 4 jet) the vector dominance related backgrounds are suppressed relative to the analogous point-like photon contributions by at least a factor of 10.

Another example in the jet case (not plotted in Fig. 16) is the comparison of 4-jet contributions from the $qq \to qq$ scattering subprocess. If the initial quarks are both from ρ-dominated photons the contribution is a factor of 10^3 below the contribution where both of the initial quarks come from the point-like photon components, as in Fig. 17a. This reflects the dominance of point-like vector-dominated components of the quark distribution in a photon. Thus

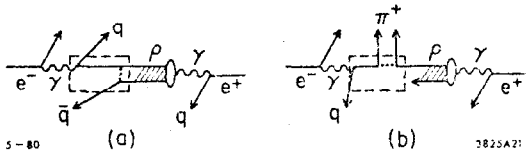

Fig. 21. Vector dominance backgrounds to (a) 2-jet production; (b) π^+ production.

even if the $\rho\rho \to$ 4-jet cross section is an unexpectedly small percentage of the calorimetric trigger rate, as appears to be the case in hadron-hadron collisions (see item (6) under Section II), it may still be that the simple point-like process $\gamma_{PL}\gamma_{PL} \to$ 4-jet will stand above the hadron-related background.

Our final vector dominance example is the contribution to single π^+ production coming from the subprocess $\gamma q \to \pi^+ q$ with the initial quark coming from a ρ-dominated photon, Fig. 21b. Figure 20 shows that this background is suppressed by a factor of ≥ 5 relative to the analogous contribution coming from $\gamma q \to \pi^+ q$ with the initial quark from a point-like photon distribution.

To summarize Section III.1 on inclusive high-p_T reactions in $\gamma\gamma$ collisions we first reemphasize that high-p_T physics is relatively clean in this situation compared to typical hadronic collisions. Possible problems are confined to:

* Non-leading-log corrections -- possibly as small as 10% for the 2-jet topology and probably about 50% for 3 and 4-jet topologies.
* Incorporating the non-zero $\langle q^2 \rangle$ of photons coming from an e^- or e^+ that is triggered on.
* Thresholds -- in leading log these effects enter through the number of photon quark components we consider. As p_T^2 increases one, for instance, passes new 2-jet $\gamma\gamma \to q\bar{q}$ thresholds when $W^2_{\text{subprocess}} \approx 4p_T^2 \geq 4m_q^2$. Effects of new quark thresholds which enter through α_s tend to cancel since α_s's cancel in most cases.

III.2. Exclusive High p_T Reactions in $\gamma\gamma$ Collisions[53]

Two photon collisions provide tests of QCD which are analogous in simplicity to, but more versatile than, those provided by form factor measurements. I will discuss briefly only two examples:

(a) $\gamma^*(Q^2)\gamma \to \pi^0$

If we define the invariant Feynman amplitude as

$$\mathcal{M} = ie^2 F_{\pi\gamma}(Q^2)\, \varepsilon_{\mu\nu\rho\sigma}\, p_\pi^\nu\, q^\rho\, \varepsilon^\sigma \quad , \tag{3.18}$$

then the exact prediction is equivalent to exposing one gluon in the π^0 wave function as in Fig. 22,

$$F_{\pi\gamma}(Q^2) \overset{Q^2 \to \infty}{\sim} \frac{2f_\pi}{Q^2} \tag{3.19}$$

with no α_s or Λ dependence in this leading order. (The PCAC constant as defined here is $f_\pi = 0.093$ GeV.) This is the same prediction as obtained many years earlier using PCAC and the Bjorken, Johnson, Low

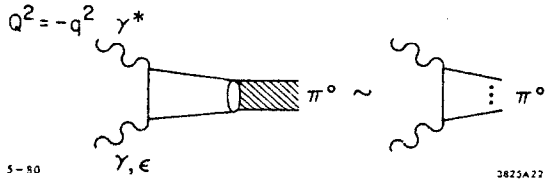

Fig. 22. Dominant diagram for $\gamma^*(Q^2)\gamma \to \pi^0$.

limit.[1] It is a fundamental and simple test of the perturbative approach to short distance physics.

(b) $\gamma\gamma \to M\bar{M}$

Here we consider only real photons. The "Born" diagrams which contribute in the large Q^2 fixed angle limit are shown in Fig. 23. After including all leading log corrections the prediction takes the form

$$\mathcal{M}_{\gamma\gamma \to M\bar{M}} = \frac{e^2\, 16\pi\, \alpha_s(Q^2)}{3}\left[\epsilon_1 \cdot \epsilon_2\, \mathcal{M}_1\left(z\,,\, \log Q^2/\Lambda^2\right)\right.$$

$$\left. + \frac{4\epsilon_1 \cdot k\, \epsilon_2 \cdot k}{Q^2}\, \mathcal{M}_2\left(z\,,\, \log Q^2/\Lambda^2\right)\right] \qquad (3.20)$$

where $z = \cos\theta_{c.m.}$ of the final M and

$$\mathcal{M}_i = \sum_{n,m} b^i_{n,m}(z)\left(\log Q^2/\Lambda^2\right)^{-\gamma_n - \gamma_m} \quad . \qquad (3.21)$$

The γ_n and γ_m are the anomalous dimensions which appear in deep inelastic scattering and the form factor prediction, Eq. (2.5), and the leading terms $b^i_{00}(z)$ are calculable in terms of the PCAC f_π. Note that the $b^i_{n,m}$'s also depend on scattering angle z so that the z dependence of the cross section can in principle be used to separate the different b's from one another.

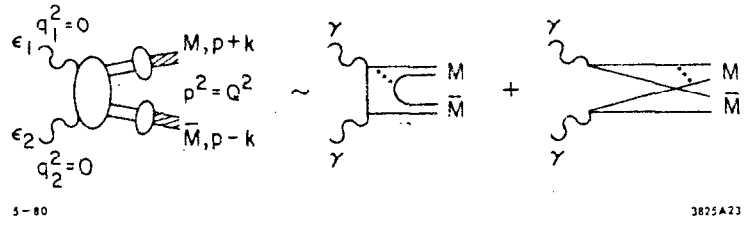

Fig. 23. Diagrams for $\gamma\gamma \to M\bar{M}$.

Again the above are fundamental yet simple predictions of QCD. These exclusive reactions may be simpler to analyze (despite their relatively small cross section) than the inclusive reactions. However, only in the inclusive reactions is it possible to directly probe the simple QCD processes $qq \to qq$, $\gamma\gamma \to q\bar{q}$, etc. Clearly both types of experiment deserve long-term attention and analysis.

IV. Conclusions

We summarize the main points of this talk.

(a) The precise low energy $\sigma_{\gamma\gamma}$ form needs more theoretical attention. It is abundantly clear that estimates of the non-Pomeron contributions to $\sigma_{\gamma\gamma}$ using vector dominance will yield only part of the answer. Additional Regge and/or fixed pole contributions, related to the point-like component of the photons, will be present.

(b) We are fortunate in the high-p_T domain to have a point-like photon component. Already experiments have seen the fundamental 2-jet signal predicted on the basis of the perturbative process $\gamma\gamma \to q\bar{q}$. In comparison hadronic collisions present a confusing picture, even refusing (according to a recent experiment) to yield a clear jet trigger signal without first biasing the event by requiring a single fast high-p_T particle.

(c) Most two-photon high-p_T predictions exhibit exact scaling and are independent of the QCD Λ parameter in leading order. All normalizations are computable. The tests of the underlying elementary-QCD cross sections are correspondingly clean.

(d) Higher twist and vector dominance related backgrounds are generally negligible except for the interesting $\gamma\gamma \to \pi^+ X$ high-p_T single particle cross section which provides a simple and fundamental measure of the normalization of an important higher-twist subprocess, $\gamma q \to \pi q$. Experimental results on $dN^{\gamma\gamma \to \pi}/dp_T^2$ will shortly provide meaningful constraints.

(e) Fundamental, but simple, QCD predictions have been obtained for several basic exclusive channels in photon-photon collisions.

Acknowledgements

I would like to thank P. Kessler and G. Parisi for their hospitality at the Amiens Two-Photon Workshop (1980) for which this talk was prepared. I would also like to thank S. J. Brodsky for communicating his recent exclusive results to me.

References

1. See M. Greco's talk at the "Workshop on Two Photon Collisions," Amiens, France (1980) and references therein.
2. F. E. Low, Phys. Rev. D12 (1975) 163; S. Nussinov, Phys. Rev. Lett. 34 (1975) 1286; J. F. Gunion and D. E. Soper, Phys. Rev. D15 (1977) 2617.
3. See the talks of Ch. Berger (PLUTO) and E. Hilger (TASSO) at the "Workshop on Two Photon Collisions," Amiens, France (1980).
4. J. F. Gunion, Phys. Lett. 88B (1979) 150.
5. V. Chang and R. Hwa, Phys. Lett. 85B (1979) 285.
6. See for example, W. R. Frazer and J. F. Gunion, Phys. Rev. D20 (1979) 147.
7. The actual prediction incorporating spin is $(1-x)^2$ + constant, $(1-x)$ is an adequate approximation over the moderate x domain. See G. Farrar and D. R. Jackson, Phys. Rev. Lett. 35 (1975) 1416.
8. The actual prediction is $\frac{(1-x)^0}{a+b\,\ell n\,(1/1-x)}$ indicating a logarithmic suppression as $x \to 1$. See Ref. 6.
9. A. M. Boyarski et al., Phys. Rev. D14 (1976) 1733. This is 18 GeV $\gamma p \to \pi^+, \pi^-$ data. Higher energy data from the tagged photon beam at FNAL will hopefully confirm this lower energy result.

10. See for example, W. Frazer and J. F. Gunion, Phys. Rev. D19 (1978) 2447 and references therein.

11. For a summary of recent progress in this area see S. J. Brodsky, SLAC-PUB-2447, presented at the Summer Institute on Particle Physics, SLAC (1979).

12. R. Blankenbecler, S. J. Brodsky and J. F. Gunion, Phys. Rev. D8 (1973) 4117; Phys. Lett. 39B (1972) 649; P. V. Landshoff and J. C. Polkinghorne, Phys. Rev. D10 (1974) 891 and references therein; M. K. Chase and W. J. Stirling, Nucl. Phys. B133 (1978) 157. For a general review see D. Sivers, R. Blankenbecler and S. J. Brodsky, Phys. Rep. 23C (1976) 1 and Ref. 11.

13. See Ref. 11 and G. P. Lepage and S. J. Brodsky, Phys. Rev. Lett. 87B (1979) 359.

14. R. K. Ellis, M. Furman, H. Haber and I. Hinchliffe, LBL-10304 (1979).

15. See L. F. Abbott and R. M. Barnett, SLAC-PUB-2227, submitted to Annals of Phys.; R. Blankenbecler and I. Schmidt, Phys. Rev. D16 (1979) 1318; W. R. Frazer and I. Schmidt, Phys. Rev. D16 (1979) 1318; W. R. Frazer and J. F. Gunion, SLAC-PUB-2489 (1980). The general form of higher twist contributions was first discussed in R. Blankenbecler, S. J. Brodsky and J. F. Gunion, Phys. Rev. D12 (1975) 3469.

16. R. M. Barnett, private communication.

17. See R. Blankenbecler, S. J. Brodsky and J. F. Gunion, Phys. Rev. D18 (1978) 900; D. Jones and J. F. Gunion, Phys. Rev. D20 (1979) 232.

18. S. D. Ellis, P. V. Landshoff and M. Jacob, Nucl. Phys. B108 (1978) 93.

19. Experimental points are from R. Stronowski, SLAC Summer Institute on Particle Physics (1979). Experimental references can be obtained there. The $\sqrt{s}$ = 31/$\sqrt{s}$ = 53 n_{eff} extractions are removed from Stronowski's graph. A different range of p_T is being probed compared to the $\sqrt{s}$ = 53/$\sqrt{s}$ = 62 extractions (at x_T = .4, p_T = 6 to 10 vs. p_T = 10 to 12). More higher twist-CIM component is expected (and seen) in the lower $\sqrt{s}$ extraction; correcting for this yields approximate agreement between the two extractions. I have also added to Stronowski's graph recent n_{eff} values obtained by the Athens, Athens, Brookhaven, CERN collaboration (A^2BC), C. Kourkoumelis et al., CERN-EP/80-07.

20. See R. P. Feynman, R. D. Field and G. C. Fox, Nucl. Phys. B128 (1979) ; Phys. Rev. D18 (1978) 3320. A variety of others have also pursued such studies. For references see Refs. 11 and 19. See also R. Field, Proceedings of the Tokyo International Conference on High Energy Physics (1978).

21. See Ref. 19 for a discussion and further references.

22. W. E. Caswell, R. Horgan and S. J. Brodsky, Phys. Rev. D18 (1978) 2415; R. Horgan and P. Scharbach, Phys. Lett. 81B (1979) 215.

23. J. F. Gunion and B. Peterson, U.C. Davis preprint UCD-79-5, Phys. Rev. to be published. Elementary QCD processes were considered in more detail by R. Baier, J. Cleymans and B. Petersson, Phys. Rev. D17 (1978) 2310.

24. H. Frisch et al., Phys. Rev. Lett. 44 (1980) 511.

25. G. R. Farrar and G. C. Fox, Rutgers preprint, RU-79-170 (1980).

26. See P. Seyboth's contribution at the Rencontre de Moriond, Les Arcs, France (1980).

27. R. M. Baltrusaitis et al., FNAL-PUB-79/38 Exp (1979); E. Amaldi et al., Nucl. Phys. B150 (1979) 326; M. Diakonov et al., CERN-EP/80-02 and 80-03.

28. R. Ruckl, S. J. Brodsky and J. F. Gunion, Phys. Rev. D18 (1978) 2469.

29. A. P. Contogouris, S. Papadopoulos and M. Hongoh, Phys. Rev. D16 (1979) 2607.

30. L. Cormell and J. F. Owens, FSU-HEP-800307 (1980).

31. S. J. Brodsky and J. F. Gunion, in progress.

32. S. J. Brodsky, T. DeGrand, J. F. Gunion and J. Weis, Phys. Rev. Lett. 41 (1978) 672; and Phys. Rev. D19 (1979) 1418.

33. C. H. Llewellyn Smith, Phys. Lett. 79B (1978) 83.

34. K. Kajantie, Phys. Scripta 29 (1979) 230; K. Kajantie and R. Raitio, Nucl. Phys. B159 (1979) 528.

35. M. Abud, R. Gatto and C. A. Savoy, Phys. Rev. D20 (1979) 2224; and Phys. Lett. 84B (1979) 229.

36. S. Berman, J. Bjorken and J. Kogut, Phys. Rev. D4 (1971) 3388.

37. See also M. Chanowitz, Proceedings of the XIIth Rencontre de Moriond (1977), edited by Tran Thanh Van; P. V. Landshoff, LEP Summer Study, 1-13 October 1978; and S. J. Brodsky and J. M. Weis, Memorial Symposium on Strong Interactions (1978), University of Washington. H. Lipkin, Nucl. Phys. B155 (1979) 104, feels that color fluctuations invalidate this result; however the contribution is basically of a "Z-graph" type (refering to time ordered perturbation theory) which would not be affected by color fluctuations. The issue is not yet settled.

38. F. Berends, Z. Kunszt and R. Gastmans, DESY preprint, DESY-80/08 (1980).

39. See the talks by Ch. Berger (PLUTO) and E. Hilger (TASSO) at the Amiens "Two-Photon Workshop (1980).

40. R. Cahn and J. F. Gunion, Phys. Rev. D20 (1979) 2253.

41. K. Kajantie and R. Raitio, Phys. Lett. 87B (1979) 133.

42. See for example, S. J. Brodsky and J. F. Gunion, Phys. Rev. Lett. 37 (1976) 402; K. Konishi, A. Ukawa and G. Veneziano, Phys. Lett. 78B (1978) 243.

43. See G. Veneziano, XIXth International Conference on High Energy Physics, Tokyo (1978).

44. A. Devoto, J. Pumplin, W. Repko and G. L. Kane, Michigan State University preprint (1979).

45. S. J. Brodsky, T. A. DeGrand and R. F. Schwitters, Phys. Lett. 79B (1978) 244.

46. See the talks by P. Kessler, G. Parisi and J. Field at the Amiens "Two-Photon Workshop" (1980) for a critical review of various approximations to $G_{\gamma/e}$. In the results quoted here I always use the equivalent photon spectrum.

47. E. Witten, Nucl. Phys. B120 (1977) 189.

48. Y. Dokshitser, D. Dyakonov and S. Troyan, SLAC-TRANS-183; R. J. DeWitt, L. Jones, J. Sullivan, D. Nillen and H. Wyld, Phys. Rev. D19 (1979) 2046.

49. W. Bardeen and A. Buras, Phys. Rev. D20 (1979) 166; D. Duke and J. Owens, Florida State University, FSU-HEP-802 401 (1980). These latter authors now agree with Bardeen and Buras.

50. T. Walsh, Amiens "Two-Photon Workshop" (1980); W. Bardeen, Lake Tahoe Two-Photon Conference (1979); W. Frazer, Lake Tahoe Two-Photon Conference (1979).

51. J. Field, E. Pietarinen and K. Kajantie, DESY preprint 79/85 (1979).

52. Actually (3.10) and (3.11) are still correct when the important $\ell n\, \ell n\, p_T^2/\ell n\, p_T^2$ corrections to $\alpha_s(p_T^2)$ are included and thus the scale invariance of (3.12) is only corrected by terms down by a full power of $\ell n\, p_T^2$.

53. This section is based on work due to S. J. Brodsky and G. P. Lepage, Ref. 11 (and references therein) and work in progress.